JACS JOURNAL OF THE AMERICAN CHEMICAL SOCIETY

Article

Cite This: J. Am. Chem. Soc. 2019, 141, 14356−14363

pubs.acs.org/JACS

Reversible Photocontrolled Nanopore Assembly

Natalie L. Mutter,[†,§] Jana Volarić,[‡,§] Wiktor Szymanski,[*,‡,∥] Ben L. Feringa,[*,‡] and Giovanni Maglia[*,†]

[†]Groningen Biomolecular Science & Biotechnology Institute and [‡]Center for Systems Chemistry, Stratingh Institute for Chemistry, University of Groningen, Nijenborg 4, 9747 AG, Groningen, Netherlands

[∥]University Medical Center Groningen, Department of Radiology, University of Groningen, Hanzeplein 1, 9713 GZ, Groningen, The Netherlands

Supporting Information

ABSTRACT: Self-assembly is a fundamental feature of biological systems, and control of such processes offers fascinating opportunities to regulate function. Fragaceatoxin C (FraC) is a toxin that upon binding to the surface of sphingomyelin-rich cells undergoes a structural metamorphosis, leading to the assembly of nanopores at the cell membrane and causing cell death. In this study we attached photoswitchable azobenzene pendants to various locations near the sphingomyelin binding pocket of FraC with the aim of remote controlling the nanopore assembly using light. We found several constructs in which the affinity of the toxin for biological membranes could be activated or deactivated by irradiation, thus enabling reversible photocontrol of pore formation. Notably, one construct was completely inactive in the thermally adapted state; it however induced full lysis of cultured cancer cells upon light irradiation. Selective irradiation also allowed isolation of individual nanopores in artificial lipid membranes. Photocontrolled FraC might find applications in photopharmacology for cancer therapeutics and has potential to be used for the fabrication of nanopore arrays in nanopore sensing devices, where the reconstitution, with high spatiotemporal precision, of single nanopores must be controlled.

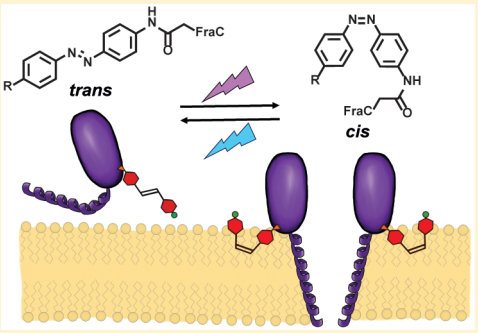

INTRODUCTION

Biological systems comprise a myriad of molecules, in which assembly, disassembly, and function must be tightly regulated. The ability to control such processes remotely using external stimuli has applications in pharmacology and biotechnology. Among the existing triggers to modulate biological activities, light is particularly attractive because it is noninvasive and allows bioorthogonal control with high spatiotemporal precision.[1−3] In the emerging field of photopharmacology, which was conceptually initiated already five decades ago,[4,5] a light-responsive small molecule,[1,6−11] most frequently an azobenzene photoswitch, is either covalently attached to the biological target or incorporated into a drug.[1,2,8,10] Azobenzene photoswitches have two isomers, the thermally stable *trans* and the metastable *cis*, which can be interconverted with light irradiation (in both directions) or by thermal relaxation (*cis* to *trans*).[10] A bioactive compound with the switch introduced into its structure is preferably nontoxic in its thermally stable state, while being activated upon irradiation with light. Despite many successful examples,[12−21] one of the main challenges remaining in the field is the lipophilic nature of the commonly used photoswitches: their introduction into the structure of known small molecule drugs leads to alteration of pharmacokinetics, solubility, and other key aspects of the bioactive molecule.

An alternative strategy involves covalent introduction of photoswitches into bioactive proteins, in particular channels and pore-forming proteins. Such proteins play an important role in living organisms for cellular communication,[22] exchange of material[23] or act as defense agents.[24] Their malfunction, or in the case of pore-forming toxins their biological function, causes disruption of cellular activity and often cell death.[25,26] Therefore, endogenous protein channels are important pharmaceutical targets.[27−29] Different approaches have been followed attempting to control channels by incorporating photoswitches.[13,30−32] Light-sensitive water-soluble small molecules were shown to act as inhibitors, causing clogging or closing of the pore.[18,33−40] Furthermore, a photoactive inhibitor was also covalently attached to the pore close to the binding site. Upon light irradiation, the photoactive ligand fits in the binding pocket, thereby closing the channel.[13,40−44] Alternatively, a photocleavable group was covalently attached into the lumen to physically block the ion flux, and upon light irradiation it was irreversibly cleaved off, rendering free passage.[45]

Rather than controlling the opening and closing of an endogenous channel, a different approach in photopharmacology involves controlling the toxicity of a pore-forming toxin

Received: July 2, 2019
Published: August 30, 2019

DOI: 10.1021/jacs.9b06998
J. Am. Chem. Soc. 2019, 141, 14356−14363

(PFT) for targeting cancer cells. PFTs are generally excreted as water-soluble monomeric polypeptides. Multiple copies of these proteins assemble on the surface of lipid bilayers to form a nanoscale water conduit that allows passage of molecules across the membrane (Figure 1A). Attempts to photoregulate

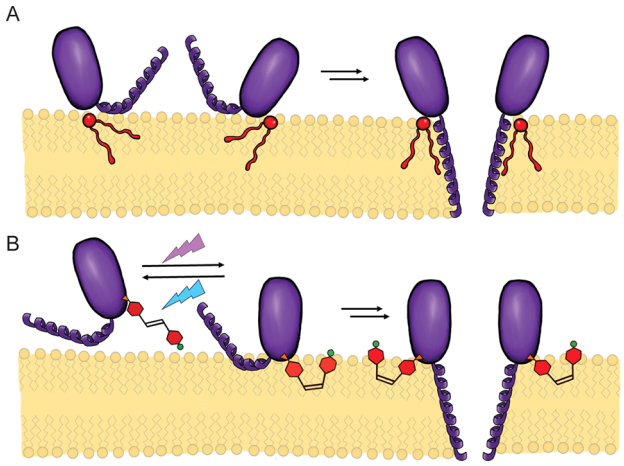

Figure 1. Assembly of photocontrolled nanopore. (A) Mechanism of FraC (purple) pore formation where sphingomyelin (red) present in the lipid bilayer (yellow) stabilizes the formed pore. (B) Proposed mechanism: FraC modified with a photoswitch (red) does not bind to the surface of the cell when the azobenzene is in the *trans* state, possibly because the charged group in the *para* position limits the affinity with the hydrophobic bilayer. The azobenzene can be reversibly switched to the *cis* state upon irradiation with light, allowing binding to the surface of the cell and formation of a pore. The mature pore structure is stabilized by the *cis*-azobenzene.

PFTs are very limited, and to the best of our knowledge in the only example α-hemolysin (αHL) PFT was modified by adding a photoremovable 2-nitrobenzyl group to cysteine residue, previously introduced into a region that was known to trigger hemolysis. Irradiation with light removed the protecting group and irreversibly activated the toxin toward red blood cells.[30] However, once activated, the protein was toxic toward all cells and additional targeting modifications[46,47] would need to be incorporated into the photoactivated construct.

Indeed, a major challenge in pharmacology, in particular for cancer drug design, is reducing off-target toxicity. Toward this end, recently we showed that the activity of a Fragaceatoxin C (FraC) PFT, which was modified to target cancer cells, could be completely suppressed by extending the transmembrane region of the protein with a polypeptide. In situ activation toward cancer cells was obtained by exposing to an endogenous cancer-specific protease.[48]

Here we present a modified FraC protein whose ability to form nanopores can be switched on and off using light (Figure 1B). This modification allows in situ activation of FraC and its subsequent deactivation as it diffuses away from the target region, enabling a possible future use of FraC in chemotherapy. Except for their potential use as therapeutics, PFT's including FraC have also been exploited for nanobiotechnological applications to sense and detect molecules at a single-molecule level.[49−54] In particular, thousands of individual nanopores are now integrated in portable and low-cost devices to sequence DNA.[55,56] The ability to control nanopore assembly with light will greatly reduce the complexity of fabrication of nanopore arrays.

RESULTS

In order to design a photocontrolled FraC nanopore, we focused on the interaction of the protein with the cell membrane. The aim was to obtain a toxin for which lipid binding was inhibited when the protein-appended photoswitch was in the resting *trans* state, while promoting lipid binding and subsequent pore formation upon photoswitching to the *cis* isomer. Nine cysteine substitutions were tested (Figure 2D). Three residues (Q130, E134, and Y138), which are part of the α2 helix of FraC, were selected because their side chains pointed directly toward the membrane. K77[57] and W112[53,58,59] were chosen because their substitution was reported to modulate hemolytic activity and membrane binding. G145, N147, and S166 were selected for their location in a loop at the protomer interface that faces the intercalated sphingomyelin lipid. Many of such residues were also close to or in direct contact with sphingomyelin (Figure 2D), a lipid molecule that triggers FraC oligomerization (Figure 1A).[59,60] Finally, G13 was chosen because it is in the transmembrane spanning helix (α1) and points toward the neighboring protomer. For the protein modification, four azobenzene switches were designed and synthesized (for full experimental details and characterization, see Supporting Figures S1−S20) for covalent attachment to a cysteine-modified FraC via a reactive chloroacetyl moiety (Figure 2A). The switches were designed with different substituents at the *para* position, where the first compound had no additional substituents (switch **A**, Figure S21), the second a methoxy group in order to improve the photoswitching properties[61] (switch **B**, Figure S22), the third a water-soluble negatively charged sulfonate group (switch **C**, Figure S23), and the last a positively charged quaternary ammonium group (switch **D**, Figure S26). The switching properties of the synthesized compounds were studied by NMR and UV−vis spectroscopy (Figure 2B and 2C, Figures S22−S28). Irradiation at λ = 365 nm switched the azobenzene moiety from the *trans* to the *cis* state, as observed by the decrease in the absorbance at λ = 355 nm and the emergence of new signals in the ^{1}H NMR spectrum (Figure 2C, peak F). The photostationary state ratio (PSS ratio), after achieving dynamic equilibrium under irradiation with 365 nm light, was then calculated by relative integration of the methylene peaks (Figure 2C, peak F). All four molecules proved to have high PSS ratios, over 90:10, when switching to the *cis* isomer (See Supporting Information). However, since switches **A** and **B** were not soluble in the attachment buffer (see SI), only switches **C** and **D** were used for further studies.

Azobenzene **C** was covalently attached to all different cysteine residues introduced in FraC (as confirmed by mass spectrometry, Figure 2F). The modified nanopores showed an additional absorbance peak at λ = 365 nm, typical for the azobenzene moiety (Figure 2E), and the reversible *trans* to *cis* isomerization could be followed upon irradiation at λ = 365 nm and white light (>450 nm). Numerous switching cycles could be performed, indicating the stability of the construct under aqueous conditions (Figure 2G). The cytotoxicity of the different constructs was tested on red blood cells (hemolytic activity) before and after activation by irradiation with λ = 365 nm light (Figure 2H and Figure S25). Modification at positions 145 and 147 (FraC-G145C-**C** and FraC-N147C-**C**, respectively) resulted in inactive molecules (i.e. they showed no hemolytic activity). Since both residues are at the

DOI: 10.1021/jacs.9b06998
J. Am. Chem. Soc. 2019, 141, 14356−14363

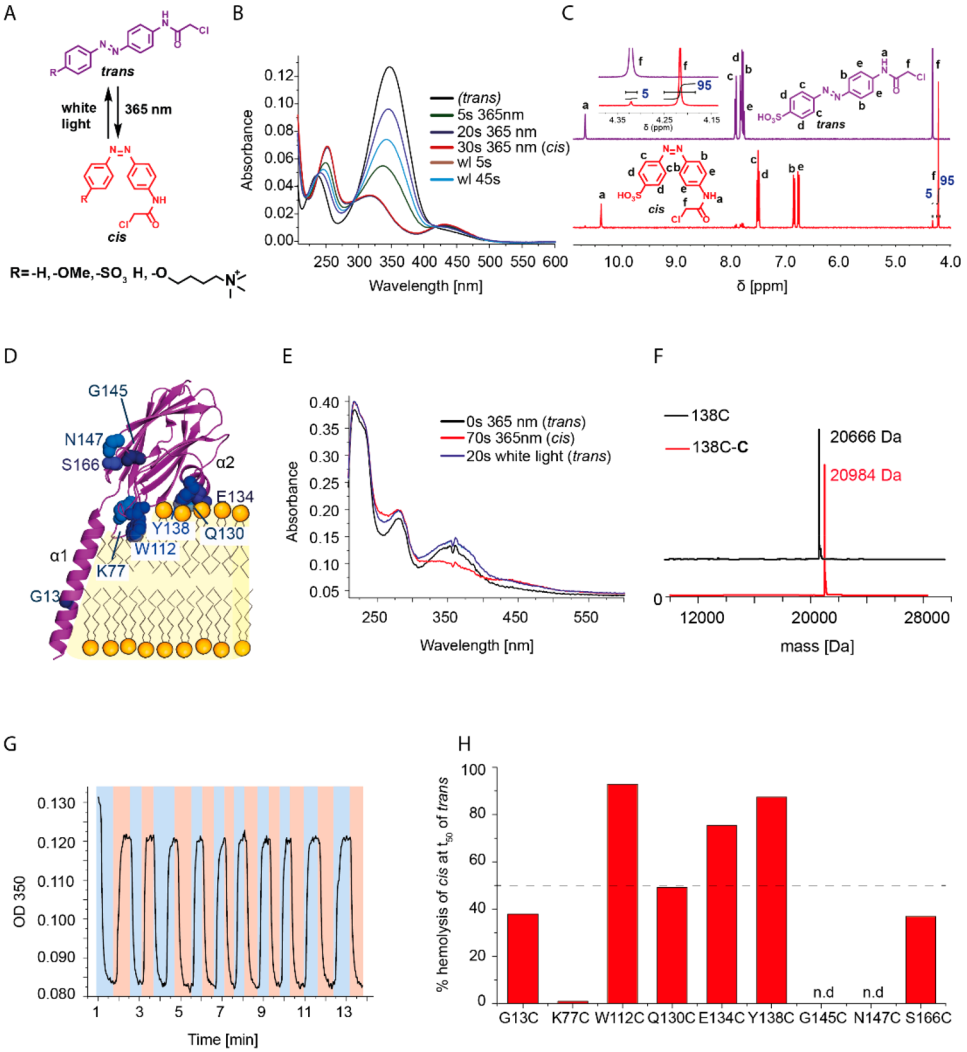

Figure 2. Engineering a light-activated toxin. (A) Chemical structures of the azobenzene switch molecules and their activation with light. (B) UV−vis spectra of switch **C** (20 μM, 25 °C) before, during irradiation at 365 nm, and after reaching the PSS state as well as back-switching with white light. Measurements were done in 150 mM NaCl, 15 mM Tris· HCl, pH 7.5. (C) ^{1}H NMR spectra of **C** (6 mM, 25 °C) in DMSO-d_6 before (*trans*, purple spectrum) and after irradiation at 365 nm (*cis*, red spectrum). (D) Cartoon representation of FraC (purple, PDB 4TSY[59]) bound to lipids (yellow), showing the amino acids substituted with cysteine (blue spheres), which were then modified by **C**. (E) UV−vis spectra of FraC-Y138C-**C** (15 μM, 25 °C) before irradiation, during irradiation at 365 nm, and after irradiation with white light. (F) ESI-MS spectra of FraC 138C and FraC-Y138C-**C**. (G) Reversible photoswitching of FraC-Y138C-**C** (15 μM, 25 °C) followed by UV−vis spectroscopy. (H) Comparison of the hemolytic activity of FraC-**C** in the *cis* or *trans* geometry. For the different FraC mutants attached to switch **C**, the bars show the % of hemolysis induced by the *cis* state at the same time point at which the *trans* state lysed 50% of the red blood cells (t_{50}). Dashed line represents the 50% level at which no selectivity of *cis* over *trans* is observed.

interface between protomers, most likely the azobenzene moiety prevented the oligomerization of FraC. For the other tested positions, the attachment of the switch to the substituted cysteine residue reduced the activity of the protein, with notable exception being the attachments at positions 130 and 134 (FraC-Q130C-**C** and FraC-E134C-**C**, respectively, Figure S29). Both residues are in the α2 helix, which resides right above the membrane (Figure 2D), suggesting that hydrophobic interactions of the α2 helix facilitate docking of FraC with the lipid bilayer. Among the variants that were hemolytically active, modifications at position 130 showed only a small difference between the *cis* and the *trans* isoforms. Modification at positions 13, 77 and 166 showed a higher cytotoxicity for the *trans* than for the *cis* isoform, while modifications at positions 112, 134 and 138 showed a faster hemolytic activity for the *cis* compared to the *trans* isoform (Figure 2H and Figure S29).

Since we aimed to obtain a toxin that is activated upon light irradiation, we selected FraC-Y138C-**C**, FraC-W112C-**C**, and FraC-E134C-**C** for further characterization. The azobenzene-modified constructs were separated from unmodified FraC using cation exchange chromatography (Figure S30A). Then the HC_{50}, which is the hemolytic concentration of toxin necessary to obtain 50% red blood cell lysis, was tested for the *cis* and *trans* isoforms.

Although all three constructs were more active in the *cis* configuration (Figure S31), FraC-Y138C-**C** showed the largest difference between the *cis* and the *trans* HC_{50} values [1.65 ± 0.10 and 6.38 ± 0.69 μM, respectively] (Figure 3A, Figures S20A and S20B). Notably, 2.2 μM FraC-Y138C-**C** showed no hemolytic activity, while irradiation with 365 nm light prior to

DOI: 10.1021/jacs.9b06998
J. Am. Chem. Soc. 2019, 141, 14356−14363

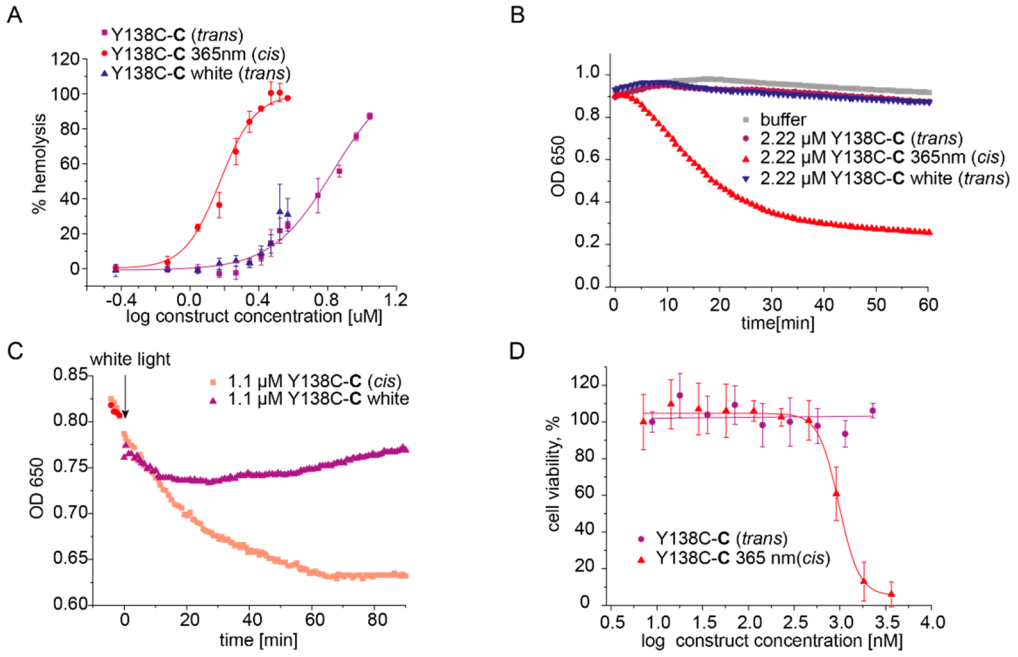

Figure 3. Light-activated toxin. (A) Comparison of the hemolysis percentage of FraC-Y138C-**C** in the *cis* state (irradiation at 365 nm, red spheres) and *trans* state (no irradiation, purple squares and irradiation with white light, blue triangles). (B) In the *trans* state (no irradiation, purple spheres) FraC-Y138C-**C** is not hemolytically active. The conversion to the *cis* state (irradiation at 365 nm, red triangles) triggers the hemolytic activity of the nanopore. Nanopore solutions first activated by irradiation at 365 nm and then deactivated with white light (blue triangles) are not hemolytically active. (C) The activity of pre-activated FraC-Y138C-pSO3 (pink squares) can be reversed by irradiation of the red blood cells with white light (purple triangles) a certain time after the beginning of the assay (red circles). (D) Toxicity of FraC-Y138C-**C** towards A431 cancer cells. Activated FraC-Y138C-**C** (irradiation at 365 nm, red triangle) is cytotoxic, while deactivated FraC-Y138C-**C** (irradiated with white light, purple spheres) does not kills the cells.

addition induced complete red blood cell lysis (Figure 3B), indicating successful design of a photocontrolled FraC nanopore. Even though we cannot exclude the presence of *trans*-labeled monomers in the formed pores, due to a high PSS ratio (95% *cis*) the vast majority of the labeled FraC monomers will be in the *cis* state. Furthermore, the activated protein could be switched off again through irradiation with white light (Figure 3B in blue). This reversibility was further expanded to the assay conditions, since active toxins could be deactivated in the presence of red blood cells by irradiation with white light in situ (Figure 3C), indicating that the cytotoxicity is reversibly controlled by light. Substitution of the negatively charged sulfonate group with a positively charged quaternary ammonium group also showed *cis* versus *trans* selectivity but did not improve the overall transition efficiency (Figure S32).

Finally, we tested the cytotoxicity of FraC-Y138C-**C** toward human cancer cells to test its usefulness as a chemotherapeutic agent. Addition of up to 1.1 μM *trans* FraC-Y138C-**C** to A431 epidermoid carcinoma cells did not cause any cell death, while an equal concentration of *cis* showed cytotoxicity [LD_{50} = 0.93 ± 0.05 μM] (Figure 3D and Figure S33). This result indicates that light-activated toxins could function toward a variety of eukaryotic cells. Furthermore, at the concentration in which the *cis* isomer showed complete killing of A431 cancer cells, the *trans* isomer did not show any hemolytic activity toward healthy red blood cells, pointing toward the usefulness of the construct in photoactivated tumor therapy. Since the activity of FraC nanopores is enhanced by the presence of sphingomyelin in the target cell membrane, the sphingomyelin-rich cells are more vulnerable to the toxin. Therefore, there is a slight difference in potency of the *cis* isomer for the cancer cells (LD_{50} = 0.93 ± 0.05 μM) and red blood cells (HC_{50}= 1.65 ± 0.10 μM). This difference is more pronounced if in the hypothetical therapeutic scenario one compares the potency toward cancer cells in the photoactivated area (*cis* isomer) with its toxicity in the nonirradiated blood pool (HC_{50} = 6.38 ± 0.69 μM).

Alongside potential use as a cancer therapeutic, FraC has been used as a single-molecule sensor. In its oligomeric form, FraC forms nanopores in artificial lipid bilayers. Under an applied transmembrane potential, the induced ionic current across single nanopores (Figure 4A) was used to identify and study single molecules, including DNA,[52] peptides, and proteins.[53,54] Most notably, arrays of thousands of nanopores are now embedded into commercial DNA sequencing devices. Insertion of a single nanopore in a sensing device, however, is a stochastic process that cannot be fully controlled. Thus, a nanopore whose bilayer insertion can be controlled with light would speed up analysis and reduce the cost of multiplexing in nanopore sensing devices. Therefore, we tested the ability of our constructs to reversibly form nanopores in lipid bilayers. It was found that the *trans* isomer of FraC-S166C-**C** (Figure S34), which showed high hemolytic activity (Figure 2H), also forms single pores, while the *trans* isomer of FraC-Y138C-**C** could not form nanopores (Figure 4B). The direct irradiation of the electrophysiology chamber with 365 nm light, forming the *cis* isomer of FraC-Y138C-**C**, activated the nanopores as shown by stepwise increases of the bilayer conductance reflecting individual insertions into the planar lipid bilayer (Figure 4C). Subsequent in situ irradiation with white light almost completely inhibited further assembly of FraC nanopores (Figures 4D and S35). By contrast, the nanopores that were already inserted in the lipid bilayer were not affected by irradiation with white light.

DOI: 10.1021/jacs.9b06998
J. Am. Chem. Soc. 2019, 141, 14356−14363

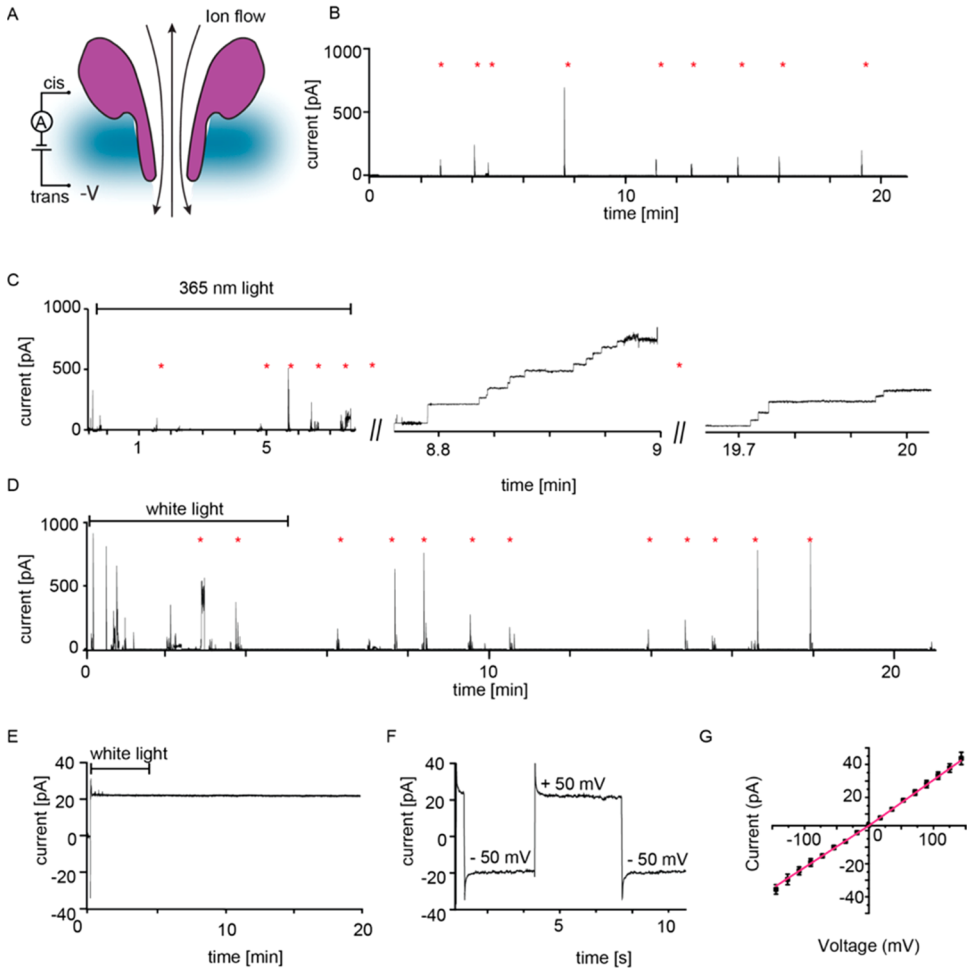

Figure 4. Light-activated nanopore. (A) Schematic representation of the nanopore experiment showing a FraC nanopore (purple) inserted in a planar lipid bilayer (blue). (B) Addition of 4 μM FraC-Y138C-**C** (*trans* conformation) to the *cis* side of an electrophysiology chamber (500 μL) did not induce the formation of nanopores, as shown by the lack of changes of the bilayer conductance. Every few minutes the bilayer was reformed (red asterisk) to ensure a stable bilayer formation. (C) About 10 min after irradiating the electrophysiology chamber with UV light at λ = 365 nm, stepwise insertions of several nanopores are observed as detected by discrete current enhancements. (D) Subsequent irradiation of the *cis* chamber (5 min, white light) prevented insertion of additional nanopores. (E) After a single FraC-Y138C-**C** was reconstituted, insertion of additional nanopores was prevented by irradiating with white light. (F and G) Relationship between current and voltage for single FraC-Y138C-**C** nanopores. Solution used for the electrical recording contained 1 M NaCl, 15 mM TrisHCl, pH 7.5. Current traces from B to E were collected applying +50 mV, a Bessel low-pass filter with 2 kHz cutoff, and sampled at 10 kHz at room temperature (25 °C).

Deactivation of FraC is advantageous in nanopore analysis because, once a single nanopore is reconstituted, irradiation with white light hinders further insertions (Figure 4E). Previously, we showed that FraC can assemble into hexameric (type III, inner constriction 0.9 nm), heptameric (type II, inner constriction 1.2 nm), and octameric (type I, inner constriction 1.6 nm) nanopores depending on the preoligomerization conditions.[53] FraC-Y138C-**C** nanopores showed a unitary conductance of 0.44 nS (+50 mV), which most likely corresponded to type III FraC nanopores (Figure 4F). This is advantageous, because type III FraC, which is the smallest nanopore characterized to date, could only be efficiently obtained at pH 4.5 but not at physiological pH.[53] Furthermore, FraC-Y138C-**C** could be assembled in the absence of sphingomyelin, and it showed a more stable conductance at positive applied potential compared to unmodified FraC nanopores (Figure 4G), suggesting that the introduced hydrophobic moiety most likely stabilized the nanopore in planar lipid bilayers.

DISCUSSION AND CONCLUSIONS

In this work we show that the assembly of the pore-forming toxin FraC from *Actinia fragacea* on lipid bilayers can be reversibly controlled by using light as an external trigger. The oligomerization of FraC nanopores is triggered by sphingomyelin, which lines the pore wall and acts as assembly cofactor.[59] Hence, we attached an azobenzene, a light-responsive molecule, to a cysteine introduced at various other positions in FraC. In particular, we selected several residues near the binding site of sphingomyelin, hoping to substitute the role of sphingomyelin as membrane anchor with the azobenzene. Azobenzenes were chosen due to their relatively high photostationary states and quantum yields as well as fast photoisomerization and low rates of photobleaching.[8,10] The azobenzene moiety was further modified by introduction of charged groups in the *para* position (sulfonate and quaternary ammonium) to increase water solubility. The additional charged group was also expected to introduce a different orientation and charge to the switch. In turn, this was anticipated to result in a differential affinity of FraC monomers

DOI: 10.1021/jacs.9b06998
J. Am. Chem. Soc. 2019, 141, 14356−14363

for the lipid membrane in the *cis* and *trans* isomeric forms. Rewardingly, we found that attachment of the azobenzene to positions near the sphingomyelin binding site granted several constructs that were inactive in the thermal resting state (*trans* azobenzene isomer) but active in the light excited state (*cis* azobenzene isomer). Interestingly, we could observe oligomerization of FraC-Y138C-**C** in the absence of sphingomyelin, suggesting that the azobenzene can substitute the sphingomyelin to promote pore formation.[60] Importantly, at selected concentrations one variant (FraC-Y138C-**C**) was completely inactive in the *trans* state while inducing full cell death in the *cis* state (Figure 3A and 3B). The cytotoxicity of photocontrolled FraC could be completely stopped by irradiation with white light (Figure 3C), hence providing reversible control of activity. There are multiple events that can be affected by the presence of the switch including binding to the surface of the target cell, oligomerization, and subsequent prepore formation or insertion of the mature pore into the lipid bilayer. Although further research is needed to precisely pinpoint the nature of photoregulation in the presented system, the observation that pores can no longer dissociate from the membrane suggests that the prepore to pore transition might not be controlled by the light switch. The azobenzene photoswitch was attached at the interface with the membrane rather than at the protomer interface; hence, a likely explanation is that the switching from *trans* to *cis* regulates the interaction with the membrane as proposed in Figure 1.

Light is an ideal external stimulus in pharmacology due to its noninvasive and biorthogonal properties as well as giving spatiotemporal control.[8,10] Hence, FraC nanopores decorated with a light-sensitive switch provide a new valuable photopharmacology tool. The reversibility of nanopore formation provides a potential use for clinical applications where the inactive toxin gets locally activated on a tumor site which is irradiated. Because of diffusion, the active monomer poses a threat to the neighboring tissue; the area around the tumor can then be irradiated with white light to switch off the diffused active toxins.

While irradiation with UV light is not ideal mainly because of the limited penetration depth, potential damage to living tissue, and interference with switching in blood,[3,62] introducing a visible light switch is the next step. Furthermore, alternative modified triggers could be introduced to further target the cytotoxicity of FraC.[48]

A light-responsive FraC might also be advantageous in biosensing applications. It has been shown that single FraC nanopores reconstituted in artificial lipid bilayers can be used to detect and study single molecules, such as DNA,[52] peptides, and proteins.[53,54] Importantly, the output signal, which is the ionic current flowing through individual nanopores, can be integrated in portable and low-cost devices containing thousands of individual pores. Here we showed that once a single nanopore is inserted, the excess of active nanopores in solution can be deactivated by irradiation with white light, greatly reducing the probability of a second insertion. In turn, this would facilitate precise preparation of arrays of single nanopores, thus reducing the cost of multiplexing.

■ ASSOCIATED CONTENT

Supporting Information

The Supporting Information is available free of charge on the ACS Publications website at DOI: 10.1021/jacs.9b06998.

Experimental details describing the synthesis, characterization, and analysis of the compounds; detailed information on mutant preparation, modification, and purification; experimental description of assays and electrical recording as well as additional figures (PDF)

■ AUTHOR INFORMATION

Corresponding Authors

*w.szymanski@umcg.nl
*b.l.feringa@rug.nl
*g.maglia@rug.nl

ORCID

Natalie L. Mutter: 0000-0002-9144-7443
Jana Volarić: 0000-0002-6198-6737
Wiktor Szymanski: 0000-0002-9754-9248
Ben L. Feringa: 0000-0003-0588-8435
Giovanni Maglia: 0000-0003-2784-0811

Author Contributions

§N.L.M. and J.V. contributed equally.

Notes

The authors declare no competing financial interest.

■ ACKNOWLEDGMENTS

We thank the University of Groningen for funding N.M., ERC consolidator grant (ID 726151) for G.M., The Netherlands Organization for Scientific Research (NWO−CW Top grant) for funding B.L.F., NWO VIDI (grant no. 723.014.001) for funding W.S., and the European Research Council (Advanced Investigator Grant no. 694345 to B.L.F.) for funding J.V.

■ REFERENCES

(1) Velema, W. A.; Szymanski, W.; Feringa, B. L. Photopharmacology: Beyond Proof of Principle. *J. Am. Chem. Soc.* **2014**, *136* (6), 2178−2191.

(2) Hüll, K.; Morstein, J.; Trauner, D. In Vivo Photopharmacology. *Chem. Rev.* **2018**, *118* (21), 10710−10747.

(3) Lerch, M. M.; Hansen, M. J.; van Dam, G. M.; Szymanski, W.; Feringa, B. L. Emerging Targets in Photopharmacology. *Angew. Chem., Int. Ed.* **2016**, *55* (37), 10978−10999.

(4) Bartels, E.; Wassermann, N. H.; Erlanger, B. F. Photochromic Activators of the Acetylcholine Receptor. *Proc. Natl. Acad. Sci. U. S. A.* **1971**, *68* (8), 1820−1823.

(5) Lester, H. A.; Krouse, M. E.; Nass, M. M.; Wassermann, N. H.; Erlanger, B. F. A Covalently Bound Photoisomerizable Agonist: Comparison with Reversibly Bound Agonists at Electrophorus Electroplaques. *J. Gen. Physiol.* **1980**, *75* (2), 207−232.

(6) Pianowski, Z. L. Recent Implementations of Molecular Photoswitches into Smart Materials and Biological Systems. *Chem. - Eur. J.* **2019**, *25* (20), 5128−5144.

(7) Wang, J.; Hou, L.; Browne, W. R.; Feringa, B. L. Photoswitchable Intramolecular Through-Space Magnetic Interaction. *J. Am. Chem. Soc.* **2011**, *133* (21), 8162−8164.

(8) Szymański, W.; Beierle, J. M.; Kistemaker, H. A. V.; Velema, W. A.; Feringa, B. L. Reversible Photocontrol of Biological Systems by the Incorporation of Molecular Photoswitches. *Chem. Rev.* **2013**, *113* (8), 6114−6178.

(9) Tochitsky, I.; Kienzler, M. A.; Isacoff, E.; Kramer, R. H. Restoring Vision to the Blind with Chemical Photoswitches. *Chem. Rev.* **2018**, *118* (21), 10748−10773.

(10) Beharry, A. A.; Woolley, G. A. Azobenzene Photoswitches for Biomolecules. *Chem. Soc. Rev.* **2011**, *40* (8), 4422−4437.

(11) Hoorens, M. W. H.; Szymanski, W. Reversible, Spatial and Temporal Control over Protein Activity Using Light. *Trends Biochem. Sci.* **2018**, *43* (8), 567−575.

DOI: 10.1021/jacs.9b06998
J. Am. Chem. Soc. 2019, 141, 14356−14363

(12) Koçer, A.; Walko, M.; Bulten, E.; Halza, E.; Feringa, B. L.; Meijberg, W. Rationally Designed Chemical Modulators Convert a Bacterial Channel Protein into a PH-Sensory Valve. *Angew. Chem., Int. Ed.* **2006**, *45* (19), 3126−3130.
(13) Fortin, D. L.; Banghart, M. R.; Dunn, T. W.; Borges, K.; Wagenaar, D. A.; Gaudry, Q.; Karakossian, M. H.; Otis, T. S.; Kristan, W. B.; Trauner, D.; et al. Photochemical Control of Endogenous Ion Channels and Cellular Excitability. *Nat. Methods* **2008**, *5* (4), 331−338.
(14) Levitz, J.; Broichhagen, J.; Leippe, P.; Konrad, D.; Trauner, D.; Isacoff, E. Y. Dual Optical Control and Mechanistic Insights into Photoswitchable Group II and III Metabotropic Glutamate Receptors. *Proc. Natl. Acad. Sci. U. S. A.* **2017**, *114* (17), E3546−E3554.
(15) Zhang, F.; Sadovski, O.; Xin, S. J.; Woolley, G. A. Stabilization of Folded Peptide and Protein Structures via Distance Matching with a Long, Rigid Cross-Linker. *J. Am. Chem. Soc.* **2007**, *129* (46), 14154−14155.
(16) Samanta, S.; Qin, C.; Lough, A. J.; Woolley, G. A. Bidirectional Photocontrol of Peptide Conformation with a Bridged Azobenzene Derivative. *Angew. Chem., Int. Ed.* **2012**, *51*, 6452−645.
(17) Ferreira, R.; Nilsson, J. R.; Solano, C.; Andréasson, J.; Grøtli, M. Design, Synthesis and Inhibitory Activity of Photoswitchable RET Kinase Inhibitors. *Sci. Rep.* **2015**, *5* (1), 9769.
(18) Volgraf, M.; Gorostiza, P.; Szobota, S.; Helix, M. R.; Isacoff, E. Y.; Trauner, D. Reversibly Caged Glutamate: A Photochromic Agonist of Ionotropic Glutamate Receptors. *J. Am. Chem. Soc.* **2007**, *129* (2), 260−261.
(19) Matera, C.; Gomila, A. M. J.; Camarero, N.; Libergoli, M.; Soler, C.; Gorostiza, P. Photoswitchable Antimetabolite for Targeted Photoactivated Chemotherapy. *J. Am. Chem. Soc.* **2018**, *140* (46), 15764−15773.
(20) Izquierdo-Serra, M.; Bautista-Barrufet, A.; Trapero, A.; Garrido-Charles, A.; Díaz-Tahoces, A.; Camarero, N.; Pittolo, S.; Valbuena, S.; Pérez-Jiménez, A.; Gay, M.; et al. Optical Control of Endogenous Receptors and Cellular Excitability Using Targeted Covalent Photoswitches. *Nat. Commun.* **2016**, *7* (1), 12221.
(21) Pittolo, S.; Gómez-Santacana, X.; Eckelt, K.; Rovira, X.; Dalton, J.; Goudet, C.; Pin, J.-P.; Llobet, A.; Giraldo, J.; Llebaria, A.; et al. An Allosteric Modulator to Control Endogenous G Protein-Coupled Receptors with Light. *Nat. Chem. Biol.* **2014**, *10* (10), 813−815.
(22) Clapham, D. E. TRP Channels as Cellular Sensors. *Nature* **2003**, *426* (6966), 517−524.
(23) Matsuzaki, T.; Tajika, Y.; Tserentsoodol, N.; Suzuki, T.; Aoki, T.; Hagiwara, H.; Takata, K. Aquaporins: A Water Channel Family. *Kaibogaku Zasshi* **2002**, *77* (2), 85−93.
(24) Peraro, M. D.; van der Goot, F. G. Pore-Forming Toxins: Ancient, but Never Really out of Fashion. *Nat. Rev. Microbiol.* **2016**, *14* (2), 77−92.
(25) Zaydman, M. A.; Silva, J. R.; Cui, J. Ion Channel Associated Diseases: Overview of Molecular Mechanisms. *Chem. Rev.* **2012**, *112* (12), 6319−6333.
(26) Kasianowicz, J. J. Introduction to Ion Channels and Disease. *Chem. Rev.* **2012**, *112* (12), 6215−6217.
(27) Gorostiza, P.; Isacoff, E. Y. Nanoengineering Ion Channels for Optical Control. *Physiology* **2008**, *23* (5), 238−247.
(28) Bregestovski, P. D.; Maleeva, G. V. Photopharmacology: A Brief Review Using the Control of Potassium Channels as an Example. *Neurosci. Behav. Physiol.* **2019**, *49* (2), 184−191.
(29) Szymański, W.; Yilmaz, D.; Koçer, A.; Feringa, B. L. Bright Ion Channels and Lipid Bilayers. *Acc. Chem. Res.* **2013**, *46* (12), 2910−2923.
(30) Chang, C.; Niblack, B.; Walker, B.; Bayley, H. A Photogenerated Pore-Forming Protein. *Chem. Biol.* **1995**, *2* (6), 391−400.
(31) Koçer, A.; Walko, M.; Meijberg, W.; Feringa, B. L. Chemistry: A Light-Actuated Nanovalve Derived from a Channel Protein. *Science* **2005**, *309* (5735), 755−758.
(32) Koçer, A.; Walko, M.; Feringa, B. L. Synthesis and Utilization of Reversible and Irreversible Light-Activated Nanovalves Derived from the Channel Protein MscL. *Nat. Protoc.* **2007**, *2* (6), 1426−1437.
(33) Mourot, A.; Tochitsky, I.; Kramer, R. H. Light at the End of the Channel: Optical Manipulation of Intrinsic Neuronal Excitability with Chemical Photoswitches. *Front. Mol. Neurosci.* **2013**, *6*, 5.
(34) Banghart, M. R.; Mourot, A.; Fortin, D. L.; Yao, J. Z.; Kramer, R. H.; Trauner, D. Photochromic Blockers of Voltage-Gated Potassium Channels. *Angew. Chem., Int. Ed.* **2009**, *48* (48), 9097−9101.
(35) Fehrentz, T.; Huber, F. M. E.; Hartrampf, N.; Bruegmann, T.; Frank, J. A.; Fine, N. H. F.; Malan, D.; Danzl, J. G.; Tikhonov, D. B.; Sumser, M.; et al. Optical Control of L-Type Ca2+ Channels Using a Diltiazem Photoswitch. *Nat. Chem. Biol.* **2018**, *14* (8), 764−767.
(36) Volgraf, M.; Gorostiza, P.; Numano, R.; Kramer, R. H.; Isacoff, E. Y.; Trauner, D. Allosteric Control of an Ionotropic Glutamate Receptor with an Optical Switch. *Nat. Chem. Biol.* **2006**, *2* (1), 47−52.
(37) Rennhack, A.; Grahn, E.; Kaupp, U. B.; Berger, T. K. Photocontrol of the Hv1 Proton Channel. *ACS Chem. Biol.* **2017**, *12* (12), 2952−2957.
(38) Leippe, P.; Winter, N.; Sumser, M. P.; Trauner, D. Optical Control of a Delayed Rectifier and a Two-Pore Potassium Channel with a Photoswitchable Bupivacaine. *ACS Chem. Neurosci.* **2018**, *9* (12), 2886−2891.
(39) Barber, D. M.; Schönberger, M.; Burgstaller, J.; Levitz, J.; Weaver, C. D.; Isacoff, E. Y.; Baier, H.; Trauner, D. Optical Control of Neuronal Activity Using a Light-Operated GIRK Channel Opener (LOGO). *Chem. Sci.* **2016**, *7* (3), 2347−2352.
(40) Bonardi, F.; London, G.; Nouwen, N.; Feringa, B. L.; Driessen, A. J. M. Light-Induced Control of Protein Translocation by the SecYEG Complex. *Angew. Chem., Int. Ed.* **2010**, *49* (40), 7234−7238.
(41) Banghart, M.; Borges, K.; Isacoff, E.; Trauner, D.; Kramer, R. H. Light-Activated Ion Channels for Remote Control of Neuronal Firing. *Nat. Neurosci.* **2004**, *7* (12), 1381−1386.
(42) Fortin, D. L.; Dunn, T. W.; Fedorchak, A.; Allen, D.; Montpetit, R.; Banghart, M. R.; Trauner, D.; Adelman, J. P.; Kramer, R. H. Optogenetic Photochemical Control of Designer K+ Channels in Mammalian Neurons. *J. Neurophysiol.* **2011**, *106* (1), 488−496.
(43) Rullo, A.; Reiner, A.; Reiter, A.; Trauner, D.; Isacoff, E. Y.; Woolley, G. A. Long Wavelength Optical Control of Glutamate Receptor Ion Channels Using a Tetra- Ortho -Substituted Azobenzene Derivative. *Chem. Commun.* **2014**, *50* (93), 14613−14615.
(44) Lemoine, D.; Habermacher, C.; Martz, A.; Mery, P.-F.; Bouquier, N.; Diverchy, F.; Taly, A.; Rassendren, F.; Specht, A.; Grutter, T. Optical Control of an Ion Channel Gate. *Proc. Natl. Acad. Sci. U. S. A.* **2013**, *110* (51), 20813−20818.
(45) Kahlstatt, J.; Reiß, P.; Halbritter, T.; Essen, L. O.; Koert, U.; Heckel, A. A Light-Triggered Transmembrane Porin. *Chem. Commun.* **2018**, *54* (69), 9623−9626.
(46) Panchal, R. G.; Cusack, E.; Cheley, S.; Bayley, H. Tumor Protease-Activated, Pore-Forming Toxins from a Combinatorial Library. *Nat. Biotechnol.* **1996**, *14* (7), 852−856.
(47) Koo, S.; Cheley, S.; Bayley, H. Redirecting Pore Assembly of Staphylococcal α-Hemolysin by Protein Engineering. *ACS Cent. Sci.* **2019**, *5* (4), 629−639.
(48) Mutter, N. L.; Soskine, M.; Huang, G.; Albuquerque, I. S.; Bernardes, G. J. L.; Maglia, G. Modular Pore-Forming Immunotoxins with Caged Cytotoxicity Tailored by Directed Evolution. *ACS Chem. Biol.* **2018**, *13* (11), 3153−3160.
(49) Majd, S.; Yusko, E. C.; Billeh, Y. N.; Macrae, M. X.; Yang, J.; Mayer, M. Applications of Biological Pores in Nanomedicine, Sensing, and Nanoelectronics. *Curr. Opin. Biotechnol.* **2010**, *21* (4), 439−476.
(50) Cao, C.; Long, Y.-T. Biological Nanopores: Confined Spaces for Electrochemical Single-Molecule Analysis. *Acc. Chem. Res.* **2018**, *51* (2), 331−341.
(51) Meng, F.-N.; Li, Z.-Y.; Ying, Y.-L.; Liu, S.-C.; Zhang, J.; Long, Y.-T. Structural Stability of the Photo-Responsive DNA Duplexes Containing One Azobenzene via a Confined Pore. *Chem. Commun.* **2017**, *53* (68), 9462−9465.

DOI: 10.1021/jacs.9b06998
J. Am. Chem. Soc. 2019, 141, 14356−14363

(52) Wloka, C.; Mutter, N. L.; Soskine, M.; Maglia, G. Alpha-Helical Fragaceatoxin C Nanopore Engineered for Double-Stranded and Single-Stranded Nucleic Acid Analysis. *Angew. Chem., Int. Ed.* **2016**, *55* (40), 12494−12498.
(53) Huang, G.; Voet, A.; Maglia, G. FraC Nanopores with Adjustable Diameter Identify the Mass of Opposite-Charge Peptides with 44 Da Resolution. *Nat. Commun.* **2019**, *10* (1), 835.
(54) Huang, G.; Willems, K.; Soskine, M.; Wloka, C.; Maglia, G. Electro-Osmotic Capture and Ionic Discrimination of Peptide and Protein Biomarkers with FraC Nanopores. *Nat. Commun.* **2017**, *8* (1), 935.
(55) Bayley, H. Nanopore Sequencing: From Imagination to Reality. *Clin. Chem.* **2015**, *61* (1), 25−31.
(56) Quick, J.; Loman, N. J.; Duraffour, S.; Simpson, J. T.; Severi, E.; Cowley, L.; Bore, J. A.; Koundouno, R.; Dudas, G.; Mikhail, A.; et al. Real-Time, Portable Genome Sequencing for Ebola Surveillance. *Nature* **2016**, *530* (7589), 228−232.
(57) Anderluh, G.; Barlic, A.; Potrich, C.; Macek, P.; Menestrina, G. Lysine 77 Is a Key Residue in Aggregation of Equinatoxin II, a Pore-Forming Toxin from Sea Anemone Actinia Equina. *J. Membr. Biol.* **2000**, *173* (1), 47−55.
(58) Hong, Q.; Gutierrez-Aguirre, I.; Barlic, A.; Malovrh, P.; Kristan, K.; Podlesek, Z.; Macek, P.; Turk, D.; Gonzalez-Manas, J. M.; Lakey, J. H.; et al. Two-Step Membrane Binding by Equinatoxin II, a Pore-Forming Toxin from the Sea Anemone, Involves an Exposed Aromatic Cluster and a Flexible Helix. *J. Biol. Chem.* **2002**, *277* (44), 41916−41924.
(59) Tanaka, K.; Caaveiro, J. M. M.; Morante, K.; González-Manãs, J. M.; Tsumoto, K. Structural Basis for Self-Assembly of a Cytolytic Pore Lined by Protein and Lipid. *Nat. Commun.* **2015**, *6*, 6337.
(60) Bakrac, B.; Gutiérrez-Aguirre, I.; Podlesek, Z.; Sonnen, A. F.-P.; Gilbert, R. J. C.; Macek, P.; Lakey, J. H.; Anderluh, G. Molecular Determinants of Sphingomyelin Specificity of a Eukaryotic Pore-Forming Toxin. *J. Biol. Chem.* **2008**, *283* (27), 18665−18677.
(61) Szymański, W.; Wu, B.; Poloni, C.; Janssen, D. B.; Feringa, B. L. Azobenzene Photoswitches for Staudinger-Bertozzi Ligation. *Angew. Chem., Int. Ed.* **2013**, *52* (7), 2068−2072.
(62) Kalka, K.; Merk, H.; Mukhtar, H. Photodynamic Therapy in Dermatology. *J. Am. Acad. Dermatol.* **2000**, *42* (3), 389−413.

DOI: 10.1021/jacs.9b06998
J. Am. Chem. Soc. 2019, 141, 14356−14363